Comparison of and correlation between anterior and posterior corneal elevation maps in normal eyes and keratoconus-suspect eyes

Zuzana Schlegel, MD, Thanh Hoang-Xuan, MD, Damien Gatinel, MD, PhD

PURPOSE: To compare the anterior and posterior corneal elevation maps between keratoconus-suspect eyes and normal eyes.

SETTING: Rothschild Foundation, AP-HP, University Paris VII, Hôpital Bichat Claude Bernard, Paris, France.

METHODS: The anterior and posterior corneal surface elevations were analyzed and compared in 60 normal myopic patients and 48 keratoconus-suspect patients. The anterior and posterior best-fit sphere radii, central and thinnest corneal pachymetries, anterior and posterior aconic shape parameters (aconic radius, aconic asphericity, aconic toricity), and anterior and posterior elevation in the 1.0 mm radius zone were analyzed. The correlations between elevation and aconic shape parameters between the anterior and posterior surfaces were compared.

RESULTS: The mean central and thinnest pachymetry values were significantly lower in keratoconus-suspect eyes ($P<.0001$). Compared with normal eyes, keratoconus-suspect eyes had significantly increased anterior toricity ($P = .0002$) and posterior toricity ($P<.0001$), more negative asphericity ($P = .042$), and higher posterior elevation ($P<.0001$). The correlation between aconic toricity and the anterior and posterior corneal surfaces was better in keratoconus-suspect eyes than in normal eyes. Aconic asphericity and apical curvature were less correlated in keratoconus-suspect eyes than in normal eyes.

CONCLUSIONS: The posterior corneal elevation and the corneal thickness values were different in keratoconus-suspect eyes. The correlation between the anterior and posterior corneal aconic shapes was between keratoconus-suspect eyes and normal eyes.

J Cataract Refract Surg 2008; 34:789–795 © 2008 ASCRS and ESCRS

The prevalence of keratoconus in the general population is approximately 1 per 2000,[1,2] and it is higher among candidates for refractive surgery[3,4] Accurate corneal measurements and imagery are essential for selecting the best corneal refractive strategies for long-term, safe visual outcomes. Proper preoperative recognition of forme fruste keratoconus patients is critical to eliminate this risk for ectasia after laser in situ keratomileusis (LASIK).[5–8]

A large analysis of anterior corneal surface topographies in eyes of refractive surgery candidates raises the possibility of a pattern continuum from isolated inferior steepening to true keratoconus. This underlines the need for further studies to identify new criteria to improve the detection of at-risk patients.

After the introduction of Placido-disk videokeratography, newer systems to analyze the anterior segment of the eye were developed. These systems include the Orbscan (Bausch & Lomb), which is based on scanning slit-beam topography; the Pentacam rotating Scheimpflug camera (Oculus); and the Galilei dual Scheimpflug analyzer (Ziemer). Corneal elevation topography generates a map of the anterior and posterior corneal surfaces. The existence of early manifestations of

Accepted for publication December 27, 2007.

From Ophthalmology, Rothschild Foundation and AP-HP Bichat-Claude Bernard Hospital, and the Center of Expertise and Research in Optics for Clinicians, Paris, France.

No author has a financial or proprietary interest in any material or method mentioned.

Corresponding author: Damien Gatinel, MD, PhD, Rothschild Foundation, 25 rue Manin, 75019 Paris, France. E-mail: gatinel@aol.com.

0886-3350/08/$—see front matter
doi:10.1016/j.jcrs.2007.12.036

keratoconus at the posterior surface or of a true independent alteration of the posterior curvature remains controversial. Studies in the early 1990s[9,10] suggested that posterior keratoconus represents distinct clinical pathology. These studies found diffuse or focal corneal thinning associated with posterior depression of the cornea and minimal or no anterior surface changes detected with the slitlamp, keratometer, or photokeratoscope. In previous studies, posterior corneal elevation characteristics were appreciated in terms of maximum elevation value, or best-fit sphere (BFS) radius value, or both. Surface height is measured relative to a symmetric and close-fitting reference surface. The corneal surface is variably aspherical and toric. Therefore, an aspherical and toric reference surface, such as an aconic surface, would lie closer to the corneal surface of interest and provide information that a reference sphere cannot.

The purpose of this study was to assess and compare the anterior and posterior surface elevation topography characteristics in keratoconus-suspect eyes using an objective automated method of detection based on independent anterior specular topography data. The anterior and posterior corneal surfaces in these eyes were analyzed using Orbscan IIz slit-scanning topography. We compared the anterior and posterior corneal shape characteristics of the same cornea in keratoconus-suspect eyes and normal eyes using spherical and nonspherical reference surfaces and then evaluated the degree of correlation.

PATIENTS AND METHODS

This retrospective review included 108 eyes (60 normal and 48 keratoconus suspect) of myopic patients seeking refractive surgery that were evaluated as part of a routine preoperative examination. Inclusion criteria included preoperative examination with the OPD-Scan Placido-based (Nidek) and Orbscan IIz Placido and slit-scanning topography systems. All patients provided informed consent.

The Orbscan IIz and OPD-Scan videokeratographs were obtained by 2 highly experienced operators. The Nidek Corneal Navigator (NCN) was used to analyze the data obtained by OPD-Scan anterior topography. The NCN uses an artificial intelligence technique in which it trains a computer neural network to recognize specific classifications of corneal topography. The NCN first calculates various indices representing corneal shape characteristics. After these indices are input, the NCN classifies the results from the neural network into 9 types: normal, astigmatism, keratoconus suspect, keratoconus, pellucid marginal degeneration, postkeratoplasty, myopic refractive surgery, hyperopic refractive surgery, and unclassified variation. These diagnostic results are estimated based on the relationship between many corneal indices and cases. For each diagnostic condition, the percentage of similarity is indicated; the value varies from 0% to 99%. The indicated result for each topography condition is independent of other categories.

There were 2 groups of patients. In the normal group, 1 eye was randomly selected from patients in whom both eyes had a score of 99% similarity to normality using the NCN analysis from the OPD-Scan specular topography data without Orbscan IIz topography patterns suggestive of forme fruste keratoconus such as focal or inferior steepening of the cornea or central keratometry greater than 47.0 diopters (D) on the Orbscan IIz map. The consecutive patients had had LASIK without ectasia complications over a minimum postoperative follow-up of 1 year.

The keratoconus-suspect group included eyes that had a positive (non-null) score for keratoconus-suspect similarity but a null score (0%) for true keratoconus similarity on NCN analysis. No eye had a history of eye disease, injury, contact lens wear, or surgery. Some were fellow eyes of patients in whom 1 eye was diagnosed as having manifest keratoconus on NCN examination. OPD-Scan or Orbscan IIz maps of the suspicious videokeratographies usually showed 1 or more of the following signs: an area of central, inferior, or superior steepening; minor topographic asymmetry; oblique cylinder greater than 1.5 D; steep keratometric curvature greater than 47.0 D; or minimum central corneal thickness less than 500 μm.

The Orbscan IIz corneal topographic maps of all eyes in both groups were assessed and reviewed. The quad map mode provided information on the anterior and posterior elevations, optical pachymetry, and axial curvature. The curvature data were obtained from the Placido data.

On the Orbscan IIz, elevation maps are plotted against a spherical reference surface whose radius and position are calculated without constraints (float mode). Other modes for elevation representation are available with the Orbscan software. The aconic mode corresponds to the representation of the corneal surface against a best-fit aconic surface (Figure 1). An aconic surface is characterized by 2 orthogonal apical radii of curvature and 2 asphericities. This allows variation of the apical curvature and asphericity of the principal meridians. As the aconic surface can be toric and aspherical, its fit is closer to the corneal surface from which it is computed. Therefore, the aconic surface provides an approximation of the overall corneal shape asphericity and toricity. From elevation data of the posterior or anterior corneal surface, the Orbscan IIz software generates an aconic surface of reference and displays its mean apical curvature, asphericity, and toricity values. The aconic mode can be easily accessed with the Orbscan IIz software via the "Elevation" menu by clicking on the "View" button on the main toolbar.

The following criteria, with Orbscan IIz notations in parentheses, were analyzed and compared using the Orbscan quad map representation: central power and radius in both anterior BFS and posterior BFS; maximum anterior elevation (MAE) and posterior elevation (MPE) value relative to the BFS in the 1.0 mm radius ring; simulated keratometry in maximum (SKmax) and minimum (SKmin) dioptric values; irregularity index at 3.0 mm (II3); central pachymetry (CP); thinnest pachymetry (TP); magnitude of the decentration of the thinnest corneal point from the corneal geometric center (DTP). All values except MAE and MPE are directly available from the "Quad Map display" mode. The MAE and MPE values can be obtained via the "Stats" menu, which is accessed by the "Tools" menu on the main toolbar. The following elevation parameters were directly displayed in the Orbscan IIz anterior aconic view and posterior aconic view, respectively: apical power/radii (AAR and PAR); positive astigmatism (AAA and PAA), and asphericity (AAQ and PAQ). As mentioned, these parameters relate to the shape of the aconic surface that corresponds to the toric

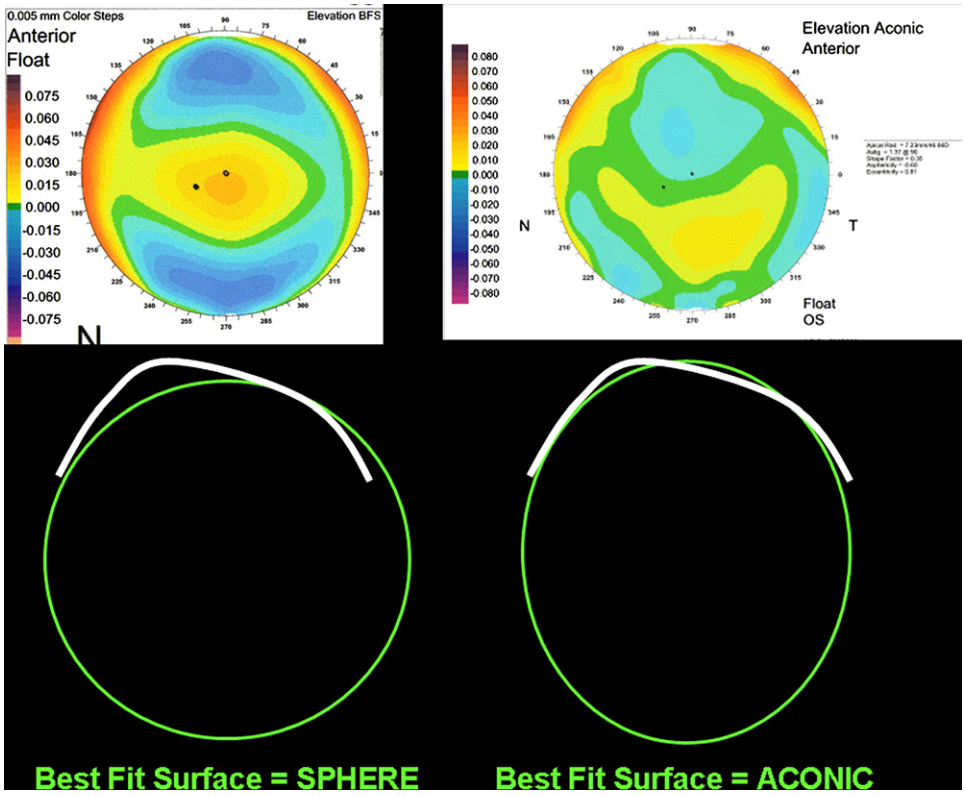

Figure 1. Best-fit sphere and aconic mode representation. The fitted aconic surface is closer than the sphere to the actual corneal shape (shown in cross sections).

and aspheric symmetrical shape that best fits the analyzed corneal surface.

All numerical results were entered into a database, and statistical analyses were performed with XLSTAT2006 (Addinsoft) using the Student *t* test. A *P* value less than 0.05) was considered statistically significant. The correlation coefficients between the anterior value and posterior value of the BFS radius, aconic radius, aconic astigmatism, aconic asphericity and 1.0 mm radius zone maximum elevation were calculated and their significance tested.

RESULTS

Of the 108 patients, 53 were men and 55 were women. Forty-eight eyes (48 patients) were diagnosed as keratoconus suspect based on the NCN automated interpretation and were eliminated from candidacy for LASIK.

Table 1. Demographic data of patients.

Characteristic	Normal Group	KS Group	*P* Value
Patients (n)	60	48	—
Eyes (n)	60	48	—
Mean age (y) ± SD	42 ± 11	34 ± 9	.01
Male sex, n (%)	15 (50)	27 (56)	.02
Mean SE (D) ± SD	−3.08 ± 2.65	−3.89 ± 2.96	.01

KS = keratoconus suspect; SE = spherical equivalent

Table 1 compares the demographic data between the 2 groups. The patients in the keratoconus-suspect group were statistically significantly younger than those in the normal group and had a statistically significantly higher mean spherical equivalent (both $P = .01$).

Table 2 shows a between-group comparison of the mean values of the 14 indices generated by Orbscan IIz topography. The differences between the keratoconus-suspect group and normal group were statistically significant for the 8 following elevation and pachymetry criteria: anterior aconic astigmatism, maximum anterior elevation, central mean and thinnest pachymetries, subtraction of mean central and thinnest pachymetries, decentration of the thinnest point, posterior aconic asphericity, posterior aconic astigmatism, and maximum posterior elevation value.

Table 3 shows the correlations between the anterior and the posterior corneal surface parameters in both groups. In the normal group, strong correlations were found between the anterior and posterior BFS radii, maximum elevations, and aconic radii values; the correlations between anterior and posterior aconic asphericity and toricity values were weak. In the keratoconus-suspect group, the BFS aconic apical radii and toricity values of the anterior and the posterior surfaces were significantly correlated, whereas the aconic asphericity and maximum elevation values were not.

Table 2. Statistical significance of comparisons of the means between normal eyes and keratoconus-suspect eyes.

Compared Orbscan Index	Mean ± SD		*P* Value
	Normal Eyes	KS Eyes	
ABFS (D)	42.74 ± 1.21	42.51 ± 1.46	.371
PBFS (D)	51.86 ± 2.04	51.73 ± 1.86	.725
CP (μm)	559.70 ± 36.10	513.52 ± 40.76	<.0001
TP (μm)	551.87 ± 36.63	502.02 ± 42.67	<.0001
CP – TP (μm)	7.83 ± 4.49	11.50 ± 22.57	<.0001
DTP (mm)	0.64 ± 0.33	0.87 ± 0.37	<.01
AAR (mm)	7.59 ± 0.36	7.64 ± 0.35	.521
AAQ	−0.32 ± 0.21	−0.36 ± 0.21	.518
AAA (D)	0.90 ± 0.54	1.43 ± 0.87	.0002
PAR (mm)	6.28 ± 0.31	6.20 ± 0.34	.175
PAQ	−0.27 ± 0.17	−0.38 ± 0.39	.042
PAA (D)	1.23 ± 0.95	2.29 ± 1.71	<.0001
MAE (mm)	0.0106 ± 0.0049	0.0133 ± 0.0050	.0057
MPE (mm)	0.0206 ± 0.0089	0.0288 ± 0.0102	<.0001

AAA = anterior aconic astigmatism; AAQ = anterior aconic asphericity; AAR = anterior aconic radius; ABFS = anterior best-fit sphere; D = diopter, CP = central pachymetry; DTP = decentration of the thinnest point; CP – TP = subtraction of two pachymetry values; KS = keratoconus suspect; MAE = maximum anterior elevation at 1.0 mm radius zone; MPE = maximum posterior elevation at 1 mm radius zonep = significance level; PAA = posterior aconic astigmatism; PAQ = posterior aconic asphericity; PAR = posterior aconic radius; PBFS = posterior best-fit sphere; TP = thinnest pachymetry

DISCUSSION

Although the introduction of computerized videokeratography increased the ability to diagnose some cases of forme fruste keratoconus, ectasia after keratorefractive surgery still occurs, even in cases of low myopic correction[11] or in patients without currently identifiable risk factors. To minimize the risk for ectasia, LASIK surgeons should avoid high myopic corrections and residual stromal beds thinner than 250 μm[12] and use intraoperative pachymetry to detect unanticipated flap errors.

Detecting clinically advanced keratoconus is not difficult. In contrast, defining topographical criteria that allow one to distinguish between keratoconus-suspect eyes and normal eyes remains problematic. At present, there are no specific or universally accepted criteria for categorizing an eye as keratoconus suspect. In some patients, anterior specular topography shows increased asymmetry, such as an inferior and localized steepening in the absence of other traditional diagnostic criteria for the keratoconus or contact lens–induced warpage. These patients can have asymmetry between the right eye and left eye (ie, reduced enantiomorphism). Patients presenting with steep keratometric readings and unstable or increasing astigmatism may have forme fruste keratoconus. In a study by Li et al.,[13] more than one third of clinically normal eyes in patients with unilateral keratoconus developed manifest keratoconus during the 8-year follow-up.

Some studies used data from anterior corneal topography only.[14–20] Numerous previous studies have tried to establish and determine a single and predictive

Table 3. Correlations between scanning slit-beam topographic indices and shape parameters between normal eyes and keratoconus-suspect eyes.

Orbscan Indices	*r* Value (95% Confidence Interval)		*P* Value	
	Normal Eyes	KS Eyes	Normal Eyes	KS Eyes
ABFS ↔ PBFS	0.839 (0.75 to 0.91)	0.665 (0.47 to 0.80)	<.0001	<.0001
AAQ ↔ PAQ	−0.233 (−0.46 to 0.02)	−0.179 (−0.44 to 0.11)	.028	.268
AAR ↔ PAR	0.360 (0.12 to 0.57)	0.324 (0.04 to 0.56)	.008	.041
AAA ↔ PAA	0.285 (0.03 to 0.5)	0.662 (0.46 to 0.80)	.0226	<.0001
MAE ↔ MPE at 1.0 mm	−0.304 (−0.52 to −0.05)	−0.285 (−0.53 to 0.00)	.001	.075

AAA = anterior aconic astigmatism; AAQ = anterior aconic asphericity; AAR = anterior aconic radius; ABFS = anterior best-fit sphere radius; KS = keratoconus suspect; MAE = maximum anterior elevation; MPE = maximum posterior elevation; PAA = posterior aconic astigmatism; PAQ = posterior aconic asphericity; PAR = posterior aconic radius; PBFS = posterior best-fit sphere radius

index that would distinguish keratoconus and keratoconus-suspect eyes from normal eyes. Fam and Lim[14] describe the anterior corneal elevation parameters such as BFS, anterior elevation, and anterior elevation ratio. Rabinowitz et al.[16–18] performed a topographical analysis to quantify the degree of anterior surface asymmetry by calculating the difference between the inferior and superior (I–S) keratometric values and degree of skewing of the steepest radial axis (SRAX). They found an I–S value of 0.8 D and an SRAX value greater than 21 degrees.

Other keratoconus-screening programs using the Rabinowitz et al.[16–18] and Maeda et al.[19,20] methods for Orbscan IIz II analysis have been proposed. Bessho et al.[21] recently proposed an automated keratoconus classifier applying a keratoconus-detection index obtained by Fourier analysis from anterior and posterior corneal surfaces and corneal thickness.

Twa et al.[22] developed an automated decision-tree classification of corneal shape through Zernike polynomial analysis. The 4 surface features selected as classification attributes by the decision-tree method were inferior elevation, greater sagittal depth, oblique toricity, and trefoil. Alió and Shabayek[23] evaluated anterior corneal surface higher-order aberrations (HOAs) to detect and grade keratoconus using corneal map analysis videokeratoscopy. They found that corneal HOAs, especially coma-like aberrations, were significantly higher in eyes with keratoconus than in normal eyes. We wonder whether such aberrations are present at the posterior corneal surface level.

Lim et al.[24] found that the mean values of maximum posterior elevation and irregularity were significantly higher in keratoconus and keratoconus-suspect eyes than in control eyes.[24]

The existence of a correlation between the radius of curvature and the asphericity of the anterior and posterior surfaces in the same patient is controversial. Tomidokoro et al.[25] found a significant positive correlation between spherical power, regular astigmatism, asymmetry, and higher-order irregularity of the anterior and posterior surfaces. These changes were also documented in keratoconus-suspect eyes, indicating involvement of the posterior surface even in the initial stage of keratoconus. Our data confirm that there is a significant difference in the maximum central posterior elevation values between keratoconus-suspect eyes and normal eyes (28.8 μm versus 20.6 μm, respectively). These values are of lesser magnitude than those reported by Lim et al.,[24] who found 26 μm and 46 μm for the maximum posterior elevation values in normal eyes and keratoconus-suspect eyes, respectively. Rao et al.[26] recommend considering a maximum central posterior elevation of 40 μm or more as a risk factor for forme fruste keratoconus. These discrepancies may be due to differences in the patients analyzed. Although NCN topography classifier allows for simultaneous non-null similarity scores for different conditions (eg, keratoconus suspect and keratoconus could have positive similarity scores in the same cornea), all eyes in our keratoconus-suspect group tested positive for keratoconus suspect but null for (manifest) keratoconus. Other authors may have used broader criteria for their form fruste keratoconus group; thus, eyes with more advanced changes toward manifest keratoconus may gave been included in the group. Our data suggest, but do not confirm, that early posterior surface changes could be occurring in patients with no symptoms and with anterior surface modifications that are so small that they would not lead to a positive identification as keratoconus suspect with automated detection.

As expected from the difference in the selection criteria, eyes in the normal group had less anterior aconic astigmatism and lower maximum elevation than eyes in the keratoconus-suspect group. The toricity of the anterior and posterior corneal surfaces had stronger significant correlations in keratoconus-suspect eyes than in normal eyes. This suggests that toricity is an important manifestation of early keratoconus-induced surface change. Unlike in the normal group, in the keratoconus-suspect group there were no significant correlations between the anterior and posterior surfaces for aconic asphericity and maximum elevation. The explanation for the reduced correlation between some anterior and posterior aconic shape parameters in keratoconus-suspect eyes deserves further investigation. Recently, we studied the effect of removal of the corneal epithelium on corneal videotopography.[27] By performing Orbscan IIz slit-scanning corneal topography before and just after corneal deepithelialization (before photoablation delivery) in myopic patients during photorefractive keratectomy, we found significant topographic differences between the air–tear film interface and Bowman layer. In particular, increased prolateness, irregularity, and toricity were seen after simple corneal epithelial debridement. This suggests that the anterior corneal epithelial layer further remodels itself in early keratoconus cases and masks or minimizes some early topographical changes at the anterior surface level. This hypothesis is compatible with our results because any increase in anterior epithelial remodeling can reduce the correlation between some anterior and posterior elevation shape characteristics in keratoconus-suspect eyes. Further studies are required to confirm this hypothesis.

A limitation of our study might be the level of reproducibility and accuracy of slit-scanning videokeratography of the posterior corneal curvature; however, a previous study[28] of measurements of the anterior

and posterior spherical powers of artificial spherical corneas showed a mean reproducibility of 0.18% and accuracy of 0.00%. In the same study, 2 consecutive measurements of the posterior surface elevation in normal eyes yielded a mean variation of 2 μm. Baek et al.[29] report reasonable accuracy in the comparative assessment of posterior corneal elevation. In eyes with keratoconus, reproducibility indices were 1.73% and 2.16% for the anterior surface and posterior surface, respectively, and were comparable to those in normal control eyes. In a recent study by Douthwaite and Mallen,[30] the Orbscan repeatability was determined and compared with that of the EyeSys videokeratoscope (EyeSys Technologies) for a set of tilted test buttons with known aspherical surface profile characteristics and for a series of measurements of normal human corneas. The Orbscan repeatability of human corneas was 0.096 mm for apical radius and 0.125 for the *P* value. Although the Orbscan appears to under-measure the apical radius and *P* values for corneal surfaces and aspherical corneas compared with the Talysurf (Taylor Hobson) and EyeSys systems, its repeatability was at least as good as that of the EyeSys (0.12 mm apical radius; 0.16 *P* value).

Corneal thinning is a key pathological feature of keratoconus. Our findings show lower mean central and thinnest point values. In addition, the difference between these values was slightly higher and the decentration of thinnest point was significantly larger in the keratoconus-suspect group than in the normal group. In contrast to our results, Rao et al.[26] did not find statistically significant differences in the mean central and thinnest point pachymetry values between keratoconus-suspect patients and a control group. However, the mean anterior and posterior elevations were more pronounced in the keratoconus-suspect group. Auffarth et al.[31] studied the subtle topographic changes in early keratoconus using the Orbscan analyzer and also found an increased distance between the corneal apex and the thinnest point in corneas with early keratoconus.

In conclusion, our data support the hypothesis that the posterior corneal surface contributes to the early topographical manifestation of keratoconus in keratoconus-suspect eyes. Although the diagnostic sensitivity was not explicitly evaluated in our study, giving more attention to posterior surface parameters may facilitate the early detection of keratoconus-suspect corneas.

REFERENCES

1. Kennedy RH, Bourne WM, Dyer JA. A 48-year clinical and epidemiologic study of keratoconus. Am J Ophthalmol 1986; 101:267–273
2. Wilson SE, Klyce SD. Screening for corneal topographic abnormalities before refractive surgery. Ophthalmology 1994; 101:147–152
3. Holland DR, Maeda N, Hannush SB, et al. Unilateral keratoconus: incidence and quantitative topographic analysis. Ophthalmology 1997; 104:1409–1413
4. Lee LR, Hirst LW, Readshaw G. Clinical detection of unilateral keratoconus. Aust N Z J Ophthalmol 1995; 23:129–133
5. Seiler T, Quurke AW. Iatrogenic keratectasia after LASIK in a case of forme fruste keratoconus. J Cataract Refract Surg 1998; 24:1007–1009
6. Amoils SP, Deist MB, Gous P, Amoils PM. Iatrogenic keratectasia after laser in situ keratomileusis for less than −4.0 to −7.0 diopters of myopia. J Cataract Refract Surg 2000; 26:967–977
7. Binder PS, Lindstrom RL, Stulting RD, et al. Keratoconus and corneal ectasia after LASIK [letter]. J Cataract Refract Surg 2005; 31:2035–2037; reply by E Donnenfeld, et al., 2037–2038
8. Rabinowitz YS, Nesburn AB, McDonnell PJ. Videokeratography of the fellow eye in unilateral keratoconus. Ophthalmology 1993; 100:181–186
9. Al-Hazzaa SAF, Specht CS, McLean IW, Harris DJ Jr. Posterior keratoconus; case report with scanning electron microscopy. Cornea 1995; 14:316–320
10. Mannis MJ, Lightman J, Plotnik RD. Corneal topography of posterior keratoconus. Cornea 1992; 11:351–354
11. Malecaze F, Coullet J, Calvas P, et al. Corneal ectasia after photorefractive keratectomy for low myopia. Ophthalmology 2006; 113:742–746
12. Binder PS. Analysis of ectasia after laser in situ keratomileusis: risk factors. J Cataract Refract Surg 2007; 33:1530–1538
13. Li X, Rabinowitz YS, Rasheed K, Yang H. Longitudinal study of the normal eyes in unilateral keratoconus patients. Ophthalmology 2004; 111:440–446
14. Fam H-B, Lim K-L. Corneal elevation indices in normal and keratoconic eyes. J Cataract Refract Surg 2006; 32:1281–1287
15. Schwiegerling J, Greivenkamp JE. Keratoconus detection based on videokeratoscopic height data. Optom Vis Sci 1996; 73:721–728
16. Rabinowitz YS. Videokeratographic indices to aid in screening for keratoconus. J Refract Surg 1995; 11:371–379
17. Rabinowitz YS, Rasheed K, Yang H, Elashoff J. Accuracy of ultrasonic pachymetry and videokeratography in detecting keratoconus. J Cataract Refract Surg 1998; 24:196–201
18. Rabinowitz YS, Rasheed K. KISA% index: a quantitative videokeratography algorithm embodying minimal topographic criteria for diagnosing keratoconus. J Cataract Refract Surg 1999; 25:1327–1335; errata 2000; 26:480
19. Maeda N, Klyce SD, Smolek MK, Thompson HW. Automated keratoconus screening with corneal topography analysis. Invest Ophthalmol Vis Sci 1994; 35:2749–2757. Available at: http://www.iovs.org/cgi/reprint/35/6/2749.pdf. Accessed February 4, 2008
20. Maeda N, Klyce SD, Smolek MK. Neural network classification of corneal topography; preliminary demonstration. Invest Ophthalmol Vis Sci 1995; 36:1327–1335. correction, 1947–1948. Available at: http://www.iovs.org/cgi/reprint/36/7/1327. Accessed February 4, 2008
21. Bessho K, Maeda N, Kuroda T, et al. Automated keratoconus detection using height data of anterior and posterior corneal surfaces. Jpn J Ophthalmol 2006; 50:409–416
22. Twa MD, Parthasarathy S, Roberts C, et al. Automated decision tree classification of corneal shape. Optom Vis Sci 2005; 82:1038–1046
23. Alió JL, Shabayek MH. Corneal higher order aberrations: a method to grade keratoconus. J Refract Surg 2006; 22:539–545

24. Lim L, Wei RH, Chan WK, Tan DTH. Evaluations of keratoconus in Asians: role of Orbscan II and Tomey TMS-2 corneal topography. Am J Ophthalmol 2007; 143:390–400
25. Tomidokoro A, Oshika T, Amano S, et al. Changes in anterior and posterior corneal curvatures in keratoconus. Ophthalmology 2000; 107:1328–1332
26. Rao SN, Raviv T, Majmudar PA, Epstein RJ. Role of Orbscan II in screening keratoconus suspects before refractive corneal surgery. Ophthalmology 2002; 109:1642–1646
27. Gatinel D, Racine L, Hoang-Xuan T. Contribution of the corneal epithelium to anterior corneal topography in patients having myopic photorefractive keratectomy. J Cataract Refract Surg 2007; 33:1860–1865
28. Oshika T, Tomidokoro A, Tsuji H. Regular and irregular refractive powers of the front and back surfaces of the cornea. Exp Eye Res 1998; 67:443–447
29. Baek TM, Lee KH, Kagaya F, et al. Factors affecting the forward shift of posterior corneal surface after laser in situ keratomileusis. Ophthalmology 2001; 108:317–320
30. Douthwaite WA, Mallen EAH. Cornea measurement comparison with Orbscan II and EyeSys videokeratoscope. Optom Vis Sci 2007; 84:598–604
31. Auffarth GU, Wang L, Völcker HE. Keratoconus evaluation using the Orbscan Topography System. J Cataract Refract Surg 2000; 26:222–228

First author:
Zuzana Schlegel, MD

Ophthalmology, Rothschild Foundation and AP-HP Bichat-Claude Bernard Hospital, and the Center of Expertise and Research in Optics for Clinicians, Paris, France